Platinum Nickel Nanowires as Methanol Oxidation Electrocatalysts

Shaun M. Alia,[a] Svitlana Pylypenko,[b] K.C. Neyerlin,[a] Shyam S. Kocha,[a,*] and Bryan S. Pivovar[a,*,z]

[a]*Chemical and Materials Science Center, National Renewable Energy Laboratory, Golden, Colorado 80401, USA*
[b]*Department of Chemistry and Geochemistry, Colorado School of Mines, Golden, Colorado 80401, USA*

Platinum (Pt) nickel (Ni) nanowires (PtNiNWs) are investigated as methanol oxidation reaction (MOR) catalysts in rotating disk electrode (RDE) half-cells under acidic conditions. Pt-ruthenium (Ru) nanoparticles have long been the state of the art MOR catalyst for direct methanol fuel cells (DMFCs) where Ru provides oxophilic sites, lowering the potential for carbon monoxide oxidation and the MOR onset. Ru, however, is a precious metal that has long term durability concerns. Ni/Ni oxide species offer a potential to replace Ru in MOR electrocatalysis. PtNiNWs were investigated for MOR and oxygen annealing was investigated as a route to improve catalyst performance (mass activity 65% greater) and stability to potential cycling. The results presented show that PtNiNWs offer significant promise in the area, but also result in Ni ion leaching that is a concern requiring further evaluation in fuel cells.
 [DOI: 10.1149/2.0231512jes]

Manuscript submitted July 7, 2015; revised manuscript received August 17, 2015. Published August 27, 2015. This was Paper 1035 presented at the Cancun, Mexico, Meeting of the Society, October 5–9, 2014.

Platinum (Pt) nickel (Ni) nanowires (PtNiNWs) have recently been developed as advanced electrocatalysts for fuel cell applications.[1] These materials have shown exceptional oxygen reduction reaction (ORR) mass activities and promising durability in rotating disk electrode (RDE) studies. These materials are also of interest in direct methanol fuel cell (DMFC) applications as a potential replacement for standard Pt-ruthenium (Ru) methanol oxidation reaction (MOR) catalysts.

High catalyst loadings and relatively high overpotential losses have limited the commercial viability of DMFCs. In addition to ORR which limits the efficiency of hydrogen fuel cells, DMFCs are also limited by the efficiency of catalysts in MOR. While DMFCs and proton exchange membrane fuel cells (PEMFCs) each use ORR catalysts at the cathode, MOR commonly requires an overpotential 300–400 mV greater than the hydrogen oxidation reaction. DMFCs typically use Pt-Ru as MOR catalysts to limit overpotential losses. Pt is effective at adsorbing methanol and partially oxidizing methanol through a number of intermediates, but is prone to carbon monoxide poisoning. Ru is typically added to provide hydroxide by hydrolysis at a lower potential than possible on Pt, lowering the methanol and carbon monoxide oxidation step through a bifunctional effect.[2–4]

Pt-Ni systems have been investigated as potential MOR catalysts, where they have shown promise in density functional theory calculations. Mavrikakis et al. and Rossmeisl et al. studied mono- and bi-metallic materials for MOR, and calculated that Pt-Ni alloys, as terraces or steps gave MOR onset potentials comparable to Pt-Ru alloys.[5–7] In experimental practice, the development of Pt-Ni alloy MOR catalysts has shown mixed results. The majority of acidic MOR studies on Pt-Ni alloys have focused on carbon-supported nanoparticles (on occasion unsupported) or electrodeposited films, finding an improvement to the peak activity, a shift in the onset to a lower potential, or improved activity in potential holds compared to carbon-supported Pt nanoparticles or Pt films.[8–13] Pt-Ni or Pt-Ni-Ru alloys have also shown improved activity compared to Pt-Ru nanoparticles or films.[14–17] Pt-Ni alloys, or the inclusion of Ni oxide, have also been used to beneficially lower the potential for carbon monoxide oxidation.[18,19] These findings, however, are not universally consistent as other studies have found no effect, or a negative effect, on the inclusion of Ni in Pt MOR catalysts.[20–22] A consensus in the literature on the effect of Ni is further complicated by the choice of benchmark catalyst (Pt-Ru nanoparticles or comparable commercial catalyst often not used), variable analysis parameters (onset versus peak activity), and the qualitative nature of catalyst comparisons (variable electrochemical protocol, reference electrodes).[23,24] The potential of Pt-Ni MOR catalysts to replace Pt-Ru remains an area of interest.

Ru as a Pt alloying element in DMFC anodes has been found to have detrimental effects when considering durability. Ru is susceptible to dissolution and crossover to the cathode; Ru crossover occurs upon cell humidification or with an applied current, and can account for cell losses as high as 200 mV.[25,26] Ru is also a Pt group metal, has a higher cost, and is less earth abundant. The use of more abundant metals, such as Ni, as a Ru replacement offers cost reduction of the catalyst layer and reduced crossover and performance losses in durability.

Pt nanotubes, templated from silver nanowires, and Pt-Ru-copper nanowires were previously synthesized as MOR catalysts by spontaneous galvanic displacement and found to offer advantages compared to nanoparticle catalysts.[27,28] In comparison to silver and copper nanowires, the Ni template differs significantly in that expected surface oxide layers can participate in the reaction and perhaps aid in resisting Ni dissolution. The benefits of extended surfaces electrocatalysis include: high specific activities; long-term durability; and long-range electronic continuity.[29] PtNiNWs also have high Pt electrochemical surface areas (ECAs), in excess of 90 $m^2\ g^{-1}$, and are potentially promising as MOR electrocatalysts if surface Ni can be stabilized to provide durable, oxophilic sites to Pt.[1]

A specific concern for PtNiNWs is Ni dissolution and contamination. If both high activity and durability can be demonstrated, then PtNiNWs can potentially displace Pt-Ru as the catalyst of choice for DMFC applications. Although Ni crossover in DMFCs is less of a concern than Ru, Ni ion contamination in PEMFC MEAs has previously limited cell performance.[30–32] Ni ion contamination may similarly limit DMFC performance through ionic contamination of the polymer electrolyte. We have explored and found success with limiting Ni dissolution rates through selective acid leaching and controlled oxidation for ORR catalysts.[32] Acid leaching is a potential route to remove excess Ni, but MOR, unlike ORR, requires surface Ni species for the bifunctional MOR mechanism (surface Ni in ORR is detrimental to performance as it blocks the active Pt sites and does not participate in ORR directly). Therefore our focus has been on controlled oxidation of the PtNiNWs to explore impacts on performance and durability. The results reported have all been in RDE where Ni dissolution is not a large concern due to the high concentration of free acid in the system. This allowed us to quantify Ni dissolution rates and catalyst performance before and after potential cycling in the absence of Ni

*Electrochemical Society Active Member.
[z]E-mail: bryan.pivovar@nrel.gov

ion contamination concerns. For fuel cell implementation, the impacts of Ni dissolution rates will require further investigation.

Experimental

NiNWs (as-received from PlasmaChem GmbH) were heated in oxygen (50% oxygen, 50% inert) to targeted annealing temperatures in a tubular furnace for 2 h. The gas was kept at a low flow rate with 500 torr of back pressure and the NiNWs were heated at a ramp rate of 10°C per min. Pt displacement of the NiNWs was then completed by previously published methods in excess potassium tetrachloroplatinate.[1]

Field emission scanning electron microscopy (FESEM) images were taken with a JEOL JSM-7000F microscope, with an EDAX Genesis used for energy dispersive X-ray spectroscopy (EDS) experiments. X-ray diffraction (XRD) patterns were taken with a Bruker D8 Discover (40 kV, 35 mA), over a 2θ range of 15–87°. Inductively coupled plasma mass spectrometry (ICP-MS) measurements were taken with a Thermo Scientific iCAP Q, calibrated to a blank and three Pt Ni standards. Each measurement was taken three times, with a dwell time of 0.15 s, and a standard deviation of less than 2%. Compositions were determined by the Pt:Ni ratio, assuming that the materials contained only Pt and Ni. In the catalysts annealed to high temperature (300 and 500°C), oxygen as NiO accounted for a significant portion of the catalyst mass; mass activities in RDE testing were therefore potentially underreported for the high temperature materials.

Electrochemical measurements were taken in a 0.1 M perchloric acid electrolyte, in a RDE half-cell equipped with a glassy carbon working electrode, a Pt mesh counter electrode, and a reversible hydrogen electrode (RHE) reference connected to the main cell by a Luggin capillary. Rotation of the working electrode was set with a modulated speed rotator (Pine Instrument Company) and measurements were taken with an Autolab single channel poteniostat (Eco Chemie, Metrohm Autolab B.V.). Inks of PtNiNWs were made at concentration of 0.2 mg ml^{-1}; 5 ml of ink contained 3.8 ml water, 1.2 ml 2-propanol, and 20 μl Nafion ionomer. An aliquot (10 μl) of ink was added to the working electrode, dried, and repeated to build the loading to 30 μg $cm_{elec}{}^{-2}$. The process was repeated after graphitized carbon nanofibers were added to the inks (60 wt%) to improve the quality of the dispersion and the ECAs of the catalysts. Carbon-supported Pt nanoparticles (Pt/HSC, 46 wt% Pt, Tanaka Kikinzoku Kogyo) and and Pt-Ru nanoparticles (PtRu/C, 50 wt% Pt, 25 wt% Ru, Johnson Matthey) were coated to loadings of 17.8 and 19.9 μg_{PGM} $cm_{elec}{}^{-2}$.

Pt ECAs were determined with carbon monoxide oxidation voltammograms, assuming a Coulombic charge of 420 μC $cm_{Pt}{}^{-2}$. The working electrode was held at 0.1 V vs. RHE for 10 min in a carbon monoxide saturated electrolyte. The potential hold continued for another 10 min during a nitrogen purge; a voltammogram starting anodically was immediately run at 20 mV s^{-1}. Pt ECAs (for PtNiNWs and Pt/HSC) were confirmed by hydrogen underpotential deposition, assuming a Coulombic charge of 210 μC $cm_{Pt}{}^{-2}$. The PtNiNW cyclic voltammograms were run at 100 mV s^{-1} in the potential range 0.025−1.4 V vs. RHE as a precaution to prevent Ni from redepositing onto Pt sites.

MOR voltammograms were completed in the potential range 0.1−1.2 V vs. RHE at 5 mV s^{-1} in a nitrogen saturated 0.1 M perchloric acid electrolyte containing 1.0 M methanol. Quasi-steady state oxidation voltammograms were then completed in the potential range 0.1–0.6 V vs. RHE at 1 mV s^{-1} to minimize the charge response due to hydrogen desorption and the double charging layer.[33] Chronoamperometry experiments were also conducted by holding catalysts at a potential of 0.5 V vs. RHE for 30 min.

Potential cycling has been used as a method for performing accelerated stress tests and the U.S. Department of Energy (DOE) has established protocols for Pt dissolution and carbon corrosion when investigating ORR catalysts.[34,35] Unfortunately, standard protocols for MOR have not been established. To try to assess durability under relevant conditions, potential cycling was performed (30,000 cycles in the range of 0.1–0.5 V vs. RHE) in an effort to quantify accelerated performance losses due to Ni dissolution compared to Ru. The cycle number was chosen (30,000) to match typical ORR durability protocols and allowed for experiments to be conducted in a time efficient manner (13.5 h). 30,000 cycles has been chosen for ORR due to the automotive application, which has longer and more variable operating requirements than DMFCs; in the absence of established DMFC protocols, 30,000 cycles was viewed as a compromise between the duration of the experiment and an adequate number of cycles to allow for reasonable comparisons between samples. The upper potential chosen (0.5 V) was anticipated to be typical of (or just slightly higher than) DMFC operation. Higher potential cycling ranges were not included since the conditions are atypical in DMFC anodes and led to a near-instantaneous loss of Ru. It is not currently known how potential cycling in this range correlates to DMFC durability tests by potential holds. The effect of low potential (0.1–0.3 V vs. RHE) on Pt and Ru stability is also not known and studies have not been completed to quantify its effect or to establish a mechanism for catalyst degradation in this range. While this method has not been verified for MOR relevance, we have applied it as a durability screening technique that is at least relevant for the specific conditions probed here.

Results

Increasing the temperature during NiNW annealing resulted in: a decreased ability for Pt to displace the NiNWs; an increase in the oxide content; and an increase in the nanowire diameter. The NiNWs, untreated or annealed, were exposed to excess Pt precursor during galvanic displacement. Heating of the NiNWs in oxygen, however, limited Pt displacement and the Pt content decreased with increasing annealing temperature (Figure 1a). EDS, taken at 5 kV to focus near the nanowire surface, also found an increasing oxide content with increasing temperature (Figure 1c). X-ray photoelectron spectroscopy found that the as-received NiNWs contained Ni hydroxide near the nanowire surface.[36] Following annealing to 200°C, Ni oxide (NiO) began to appear and replaced the Ni hydroxide response by 300°C. XRD patterns of the as-synthesized PtNiNWs showed peaks indicating distinct Pt (39.8°) and Ni (44.5, 51.9, and 76.5°) metal peaks (Figure 1b). Although the untreated NiNWs were previously shown to contain an oxide coating, the oxide did not appear in the XRD experiments.[1] A clear oxide peak became apparent for annealing at 300°C (XRD peaks at 37.1, 42.9, and 62.4°). By 500°C, Ni oxide peaks exhibited stronger signals and no Ni metal response remained. While Ni hydroxide and Ni oxide may have been present in the XRD patterns as an amorphous phase, it was also possible that the phases were crystalline but too small in quantity relative to the Ni metal in the nanowire core. Although Ni metal transitioned to NiO, the Pt maintained a "pure" Pt lattice (lattice constant 3.92 Å) regardless of temperature. Untreated PtNiNWs were 200–300 nm in diameter and ∼200 μm in length (Figure 2). Although annealing to low temperature did not appreciably change the morphology, at higher temperature (300 and 500°C), the diameter increased to 400–600 nm. The increased diameter may have been due to the expected molar volume change (Ni metal to NiO, 70% increase) and/or nanowire aggregation or growth, although the former proposed mechanism seems more viable for the temperatures and time frames reported.

Figures 1 and 2 contain contextual information for the electrochemical data discussed throughout the paper, confirming the presence of oxide species and providing key information to explaining how oxidative treatments modify the MOR activity of PtNiNWs. Annealing Ni to improve the MOR activity of Pt involved trade-offs: annealing increased the stability of surface Ni, reducing the potential for methanol and intermediate oxidation; but annealing decreased the extent of Pt displacement and the amount of Pt available to oxidize methanol. Oxidative treatments decreased the MOR onset potential and at moderate temperature (200 and 300°C), the onset was slightly lower than PtRu/C (Figure 3a). A similar shift in peak MOR activity was also observed, where increasing the annealing temperature resulted in a gradual shift in peak activity to lower potential (Figure 3b).

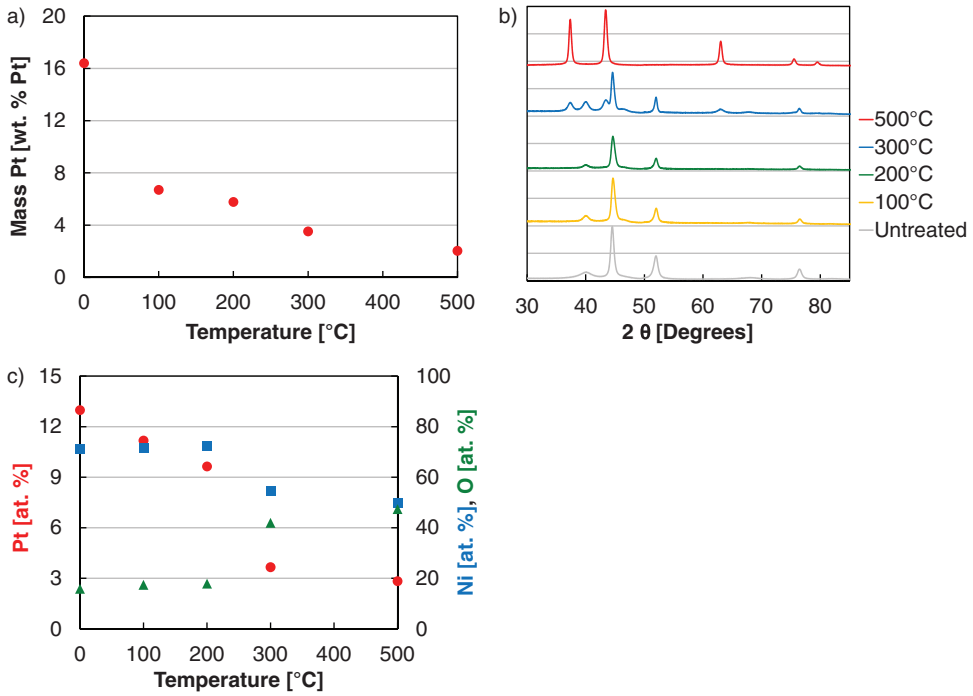

Figure 1. (a) ICP-MS, (b) XRD, and (c) EDS data at 5 kV of PtNiNWs. Data from the PtNiNWs synthesized from the untreated NiNWs was included at 0°C.

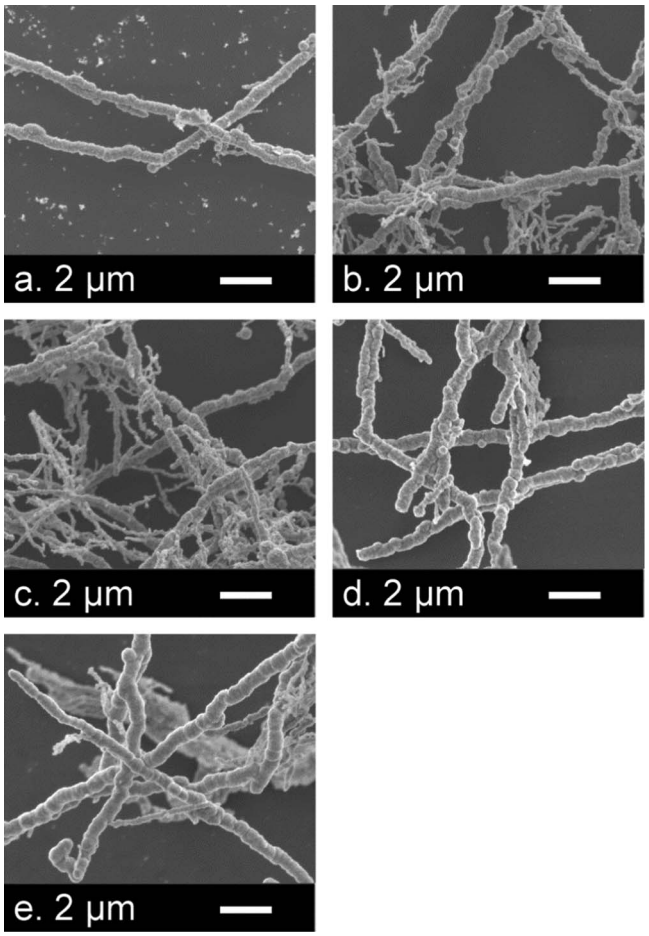

Figure 2. SEM images of PtNiNWs. NiNWs were (a) untreated and annealed in oxygen to (b) 100, (c) 200, (d) 300, and (e) 500°C prior to attempting maximum Pt displacement.

Increasing temperature, however, also resulted in lower peak activity, although this metric is less important than activity at low potential. The results were also similar to those observed in carbon monoxide oxidation, where annealing to higher temperature reduced the potential for oxidation (Figure 3c). Annealing to moderate temperature also allowed for the PtNiNWs to retain higher activity than PtRu/C in chronoamperometry experiments, indicating an improved ability to oxidize intermediates at low potential (Figure 3d). Annealing to 200°C resulted in the highest performing PtNiNW: higher MOR activity than PtRu/C throughout the onset region; higher peak activity; and improved retention of activity in chronoamperometry tests.

XRD patterns confirmed a characteristically Pt lattice and was consistent with previously microscopy of relatively segregated Pt and Ni zones in close proximity.[1] For untreated PtNiNWs and those annealed to 100°C, small amounts of Ni persisted at the surface following acid exposure. Responses in carbon monoxide and MOR showed a peak characteristic of pure Pt and a shoulder at lower potential (a second peak in carbon monoxide); the observed activity at lower potential may have been due to small amounts of Ni that remained at the surface. Upon higher annealing temperatures (200 and 300°C), greater amounts of Ni persisted following acid exposure and the MOR and carbon monoxide responses shifted to lower potential. Although secondary peaks were not observed, broad shoulders were found stretching into higher potentials. These shoulders potentially indicated variety in the degree of Pt's access to Ni and oxophillic species.

MOR activity following potential cycling demonstrates perhaps the largest prospective benefit of the PtNiNWs. Potential cycling PtRu/C leached Ru by electrochemical dissolution ($Ru \rightarrow Ru^{2+}$, 0.45 V vs. RHE), shifting methanol and carbon monoxide oxidation to higher potentials. Activity in chronoamperometry dropped, as well, indicating a declining ability to oxidize intermediates at low potential. In comparison, PtNiNWs annealed to moderate temperature maintained a high level of MOR activity following potential cycling. Although positive potential shifts were observed, they were less severe than the commercial benchmark (Figure 4a). Small losses in peak PtNiNW MOR activity were also found, but the potential shifts were also significantly smaller than those of PtRu/C (Figure 4b). Similar results were observed in carbon monoxide oxidation, where the potential shift was smaller than the commercial benchmark (Figure 4c). In chronoamperometry testing, the annealed PtNiNWs exhibited slightly larger

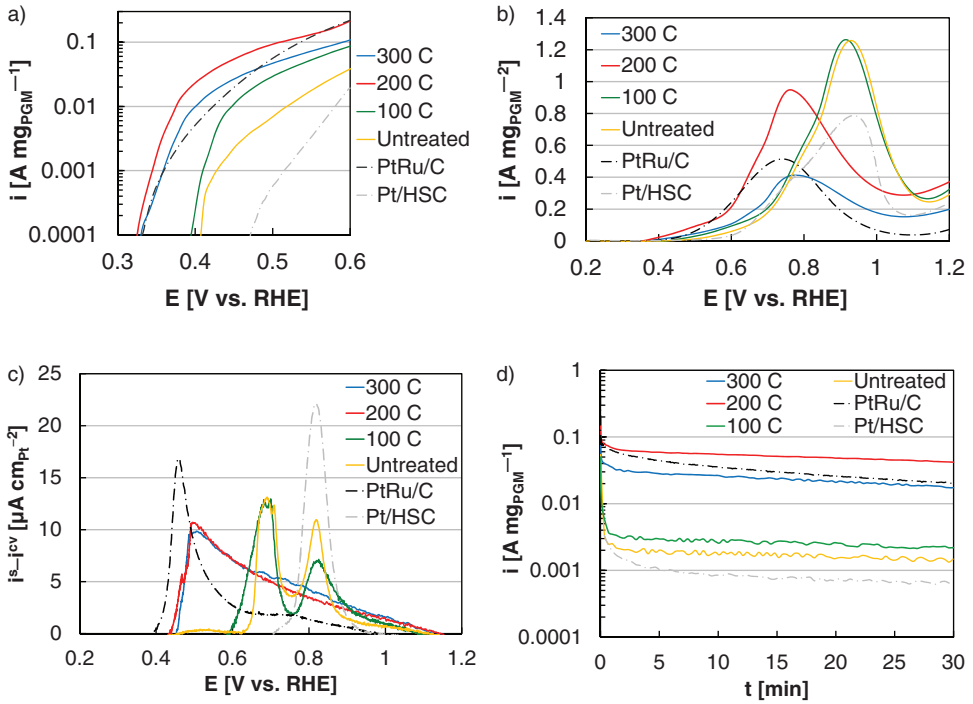

Figure 3. MOR and carbon monoxide oxidation data of PtNiNWs, PtRu/C, and Pt/HSC. (a) Quasi-steady state oxidation voltammograms at 1 mV s^{-1}, (b) anodic linear sweep voltammograms at 5 mV s^{-1}, (c) carbon monoxide oxidation voltammograms at 20 mV $^{-1}$, and (d) chronoamperometry potential holds (30 min) at 0.5 V vs. RHE.

activity losses (Figure 4d) than the same catalysts prior to potential cycling (Figure 3d). The results, however, show a significantly improved performance relative to PtRu/C, where potential cycling dramatically reduced activity, to a level comparable to Pt/HSC. Annealing to higher temperature reduced Ni dissolution rates, likely improving the stability of the PtNiNWs and their ability to maintain MOR activity following potential cycling (Table I). ICP-MS was taken of electrolytes following acid exposure (electrochemical break-in) and potential cycling. Annealed PtNiNWs retained a high level of activity following potential cycling, likely due to the oxidative treatments

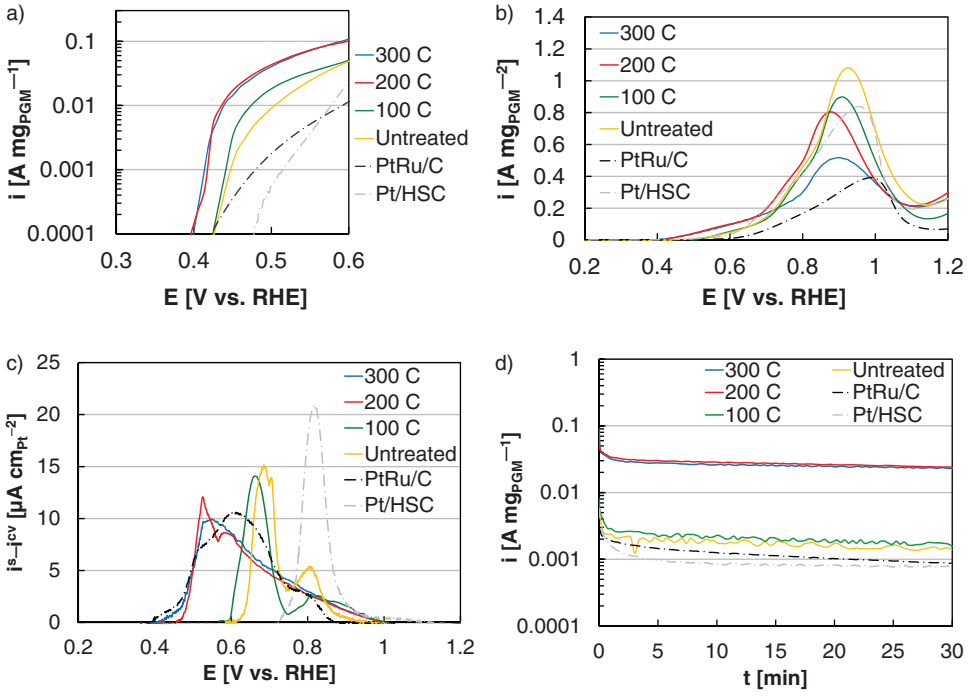

Figure 4. MOR and carbon monoxide oxidation data of PtNiNWs, PtRu/C, and Pt/HSC following potential cycling. (a) Quasi-steady state oxidation voltammograms at 1 mV s^{-1}, (b) anodic linear sweep voltammograms at 5 mV s^{-1}, (c) carbon monoxide oxidation voltammograms at 20 mV $^{-1}$, and (d) chronoamperometry potential holds (30 min) at 0.5 V vs. RHE. Accelerated stress tests were completed by potential cycling (30,000 cycles) in the range 0.1–0.5 V vs. RHE.

Table I. MOR mass activities (i_m) at 0.5 V vs. RHE, the MOR onset potential (E_O), ECA, and Ni and Ru dissolution rates (following acid exposure, denoted AE, and after potential cycling, denoted PC) prior to and following potential cycling.

	$i_{m,i}$ [A g_{PGM}^{-1}]	$i_{m,f}$ [A g_{PGM}^{-1}]	Δi_m [%]	$E_{O,i}$ [V vs RHE]	$E_{O,f}$ [V vs RHE]	ΔE_O [mV]	ECA_i [m^2 g_{PGM}^{-1}]	Ni_{AE}, Ru_{AE} [%]	Ni_{PC}, Ru_{PC} [%]
Untreated	7.0	9.1	+31	0.407	0.426	+19	41.5	2.1	0.6
100°C	29.7	18.3	−38	0.395	0.424	+30	36.6	1.6	0.3
200°C	94.1	43.7	−54	0.325	0.396	+71	28.6	0.8	0.1
300°C	47.6	40.7	−14	0.330	0.399	+69	59.2	0.5	0.1
PtRu/C	56.9	1.8	−97	0.332	0.423	+91	62.2	9.3	43.1
Pt/HSC	0.6	0.6	−2	0.471	0.477	+6	102.1	–	–

stabilizing Ni, reducing the susceptibility of Ni dissolution in RDE tests.

Annealing the PtNiNWs in oxygen stabilized surface Ni and significantly benefitted MOR activity. Surface Ni provided oxophilic species in close proximity to Pt sites, replacing the need for Ru. There may also be a benefit to using Ni in place of Ru, since Ni at the surface is an oxide in the potential window of operation where Ru is a metal more oxophilic than Pt. Thermal annealing in oxygen increased the thickness of the oxide layer, reduced Ni dissolution, and allowed for Ni to persist near the nanowire surface. Increasing the thickness of the oxide layer may provide a benefit in MOR compared to metals with adsorbed oxygen species on the surface. The exact impact or mechanism of separate oxygen species on the surface of Ni ($Ni(OH)_2$ or NiO) or thicker layers of NiO on MOR, however, was unknown; the impact of the crystallinity of those phases was also unknown.

Although the presence of surface Ni provided the largest benefit to the MOR activity of PtNiNWs, previous publications have examined a variety of other factors that may influence MOR activity on Pt. These other factors were likely minor, but are presented here to be thorough and since they may influence activity in similar systems. Pt lattice compression was previously shown to improve MOR activity by weakening Pt-OH and Pt-CO binding; in the case of PtNiNWs, however, no lattice compression was observed during XRD experiments.[7] The exposure of specific Pt facets may also influence activity.[37] In the formation of PtNiNWs, however, no effort was made to actively control Pt orientation or surface faceting.[1]

Conclusions

Annealing the NiNWs in oxygen to increasing temperature: reduced Ni dissolution rates following acid exposure and potential cycling; lowered the onset for MOR on the PtNiNWs; and improved catalyst stability in potential cycling, particularly at low overpotential. High MOR activity at the onset was achieved at the expense of peak activity and at temperatures greater than 200°C, the initial mass activity near the MOR onset began to decline as well. Data from this paper is summarized in Table I to make comparisons between individual samples and their measured electrochemical properties.

Annealing the NiNWs to 200°C resulted in the highest MOR performance. At 0.5 V vs. RHE, the annealed catalyst produced a mass activity 65% greater than PtRu/C. Following potential cycling, the activity of the PtNiNWs was more than 24 times greater. Although the MOR onset shifted to a higher potential, the shift (+71 mV) was less than that of PtRu/C (+91 mV). In comparison to the untreated material, annealing also reduced Ni dissolution by half. Annealing of the NiNWs to 300°C resulted in a tradeoff of initial MOR activity for improved stability, when compared to the 200°C material. Although the MOR activity was 49% lower, the loss after potential cycling was only 14% (compared to 54%). Ni dissolution was further reduced at 300°C and was the lowest of the synthesized materials.

The role of Ni as a contaminant must be considered upon MEA incorporation. We have previously found that the inclusion of Ni in MEA cathodes can affect PEMFC performance.[31] Although the oxygen annealing used in this study reduced Ni dissolution rates, the dissolution of Ni is still a concern in DMFC performance and must be accounted for in the MEA. At this time, the effect of Ni dissolution in the MEA has not been investigated; further tuning of catalyst content and treatment conditions will likely be required to optimize DMFC performance.

References

1. S. M. Alia, B. A. Larsen, S. Pylypenko, D. A. Cullen, D. R. Diercks, K. C. Neyerlin, S. S. Kocha, and B. S. Pivovar, *ACS Catalysis*, **4**, 1114 (2014).
2. H. A. Gasteiger, N. Markovic, P. N. Ross, and E. J. Cairns, *The Journal of Physical Chemistry*, **97**, 12020 (1993).
3. O. Petrii, *J Solid State Electrochem*, **12**, 609 (2008).
4. N. Erini, P. Krause, M. Gliech, R. Yang, Y. Huang, and P. Strasser, *Journal of Power Sources*, **294**, 299 (2015).
5. P. Ferrin and M. Mavrikakis, *Journal of the American Chemical Society*, **131**, 14381 (2009).
6. P. Ferrin, A. U. Nilekar, J. Greeley, M. Mavrikakis, and J. Rossmeisl, *Surface Science*, **602**, 3424 (2008).
7. G. A. Tritsaris and J. Rossmeisl, *The Journal of Physical Chemistry C*, **116**, 11980 (2012).
8. Y. Hu, P. Wu, Y. Yin, H. Zhang, and C. Cai, *Applied Catalysis B: Environmental*, **111–112**, 208 (2012).
9. R. S. Amin, R. M. A. Hameed, K. M. El-Khatib, M. E. Youssef, and A. A. Elzatahry, *Electrochimica Acta*, **59**, 499 (2012).
10. S. Papadimitriou, S. Armyanov, E. Valova, A. Hubin, O. Steenhaut, E. Pavlidou, G. Kokkinidis, and S. Sotiropoulos, *The Journal of Physical Chemistry C*, **114**, 5217 (2010).
11. J. Mathiyarasu, A. M. Remona, A. Mani, K. L. N. Phani, and V. Yegnaraman, *J Solid State Electrochem*, **8**, 968 (2004).
12. Y. Zhao, Y. E, L. Fan, Y. Qiu, and S. Yang, *Electrochimica Acta*, **52**, 5873 (2007).
13. Y. Hu, P. Wu, H. Zhang, and C. Cai, *Electrochimica Acta*, **85**, 314 (2012).
14. X. Wang, H. Wang, R. Wang, Q. Wang, and Z. Lei, *J Solid State Electrochem*, **16**, 1049 (2012).
15. T. Page, R. Johnson, J. Hormes, S. Noding, and B. Rambabu, *Journal of Electroanalytical Chemistry*, **485**, 34 (2000).
16. K.-W. Park, J.-H. Choi, B.-K. Kwon, S.-A. Lee, Y.-E. Sung, H.-Y. Ha, S.-A. Hong, H. Kim, and A. Wieckowski, *The Journal of Physical Chemistry B*, **106**, 1869 (2002).
17. J.-H. Choi, K.-W. Park, B.-K. Kwon, and Y.-E. Sung, *Journal of The Electrochemical Society*, **150**, A973 (2003).
18. M. Ahmadi, F. Behafarid, C. Cui, P. Strasser, and B. R. Cuenya, *Acs Nano*, **7**, 9195 (2013).
19. C. Cui, M. Ahmadi, F. Behafarid, L. Gan, M. Neumann, M. Heggen, B. R. Cuenya, and P. Strasser, *Faraday discussions*, **162**, 91 (2013).
20. J. F. Drillet, A. Ee, J. Friedemann, R. Kötz, B. Schnyder, and V. M. Schmidt, *Electrochimica Acta*, **47**, 1983 (2002).
21. E. Antolini, J. R. C. Salgado, and E. R. Gonzalez, *Journal of Power Sources*, **155**, 161 (2006).
22. H. Yang, C. Coutanceau, J.-M. Léger, N. Alonso-Vante, and N. ClaudeLamy, *Journal of Electroanalytical Chemistry*, **576**, 305 (2005).
23. E. Antolini, J. R. C. Salgado, and E. R. Gonzalez, *Applied Catalysis B: Environmental*, **63**, 137 (2006).
24. E. Antolini, *Applied Catalysis B: Environmental*, **74**, 337 (2007).
25. P. Piela, C. Eickes, E. Brosha, F. Garzon, and P. Zelenay, *Journal of The Electrochemical Society*, **151**, A2053 (2004).
26. Y. Kim and P. Zelenay, in *Polymer Electrolyte Fuel Cell Durability*, F. Büchi, M. Inaba, and T. Schmidt Editors, p. 223, Springer New York (2009).
27. S. Alia, G. Zhang, D. Kisailus, D. Li, S. Gu, K. Jensen, and Y. Yan, *Advanced Functional Materials*, **20**, 3742 (2010).
28. P. Zelenay, Advanced Materials and Concepts for Portable Power Fuel Cells, in, U. S. Department of Energy Editor, http://www.hydrogen.energy.gov/pdfs/review12/fc091_zelenay_2012_o.pdf (2012).
29. S. M. Alia, Y. S. Yan, and B. S. Pivovar, *Catalysis Science & Technology*, **4**, 3589 (2014).
30. R. Borup, J. Meyers, B. Pivovar, Y. S. Kim, R. Mukundan, N. Garland, D. Myers, M. Wilson, F. Garzon, D. Wood, P. Zelenay, K. More, K. Stroh, T. Zawodzinski, J. Boncella, J. E. McGrath, M. Inaba, K. Miyatake, M. Hori, K. Ota, Z. Ogumi, S. Miyata, A. Nishikata, Z. Siroma, Y. Uchimoto, K. Yasuda, K.-i. Kimijima, and N. Iwashita, *Chemical reviews*, **107**, 3904 (2007).

31. B. S. Pivovar, Extended, Continuous Pt Nanostructures in Thick, Dispersed Electrodes, in, U. S. Department of Energy Editor, http://www.hydrogen.energy.gov/pdfs/review14/fc007_pivovar_2014_o.pdf (2014).
32. B. Pivovar, Extended, Continuous Pt Nanostructures in Thick, Dispersed Electrodes, in, U. S. Department of Energy Editor, http://www.hydrogen.energy.gov/pdfs/review15/fc007_pivovar_2015_o.pdf (2015).
33. A. Kowal, M. Li, M. Shao, K. Sasaki, M. B. Vukmirovic, J. Zhang, N. S. Marinkovic, P. Liu, A. I. Frenkel, and R. R. Adzic, *Nat Mater*, **8**, 325 (2009).
34. M. Uchimura, S. Sugawara, Y. Suzuki, J. Zhang, and S. S. Kocha, *ECS Transactions*, **16**, 225 (2008).
35. S. S. Kocha, in *Polymer Electrolyte Fuel Cell Degradation*, M. Mench, E. C. Kumbur, and T. N. Veziroglu Editors, p. 89, Academic Press, Waltham (2011).
36. B. Pivovar, Extended, Continuous Pt Nanostructures in Thick, Dispersed Electrodes, in, U. S. Department of Energy Editor, http://www.hydrogen.energy.gov/pdfs/review14/fc007_pivovar_2014_o.pdf (2014).
37. E. Herrero, K. Franaszczuk, and A. Wieckowski, *The Journal of Physical Chemistry*, **98**, 5074 (1994).